SvedbergOpen
DISSEMINATION OF KNOWLEDGE

International Journal of Artificial Intelligence and Machine Learning

Publisher's Home Page: https://www.svedbergopen.com/

Research Paper Open Access

CFD-Based Comparative Investigation of Smooth and Hybrid Roughened Absorber Plates in a Solar Air Heater

Mr. Himanshu Pandya[1*], Dr. Pankaj Mohan Rastogi[2], Prof. (Dr.) Naveen Kumar[3], Dr. Arvind Sharma[4]

[1,2,3,4] Faculty of Integrated & Advanced Technology, Mechanical Engineering, SPSU Rajasthan.
*Corresponding Author: erhimanshupandya@gmail.com

Abstract
The present study investigates the comparatives of smooth and hybrid roughened absorber plate in solar air heater (SAH). CFD analysis of both the plates has been performed using Ansys software. Three-dimensionalCFD model was developed to investigate the thermo-hydraulic performance (THPP). The turbulence model SSTk–ω has been applied with a constant heat flux and the Reynolds number(Re) ranged 1100-5100. The analyses of flow and thermal behavior have been analyzed using velocity, temperature, and pressure contours. Further the Nusselt number (Nu), friction factor(f), and THPP has been calculated based on the CFD results.It has been observed from the results that the hybrid roughened absorber plate depicts the improved heat transfer than the baseline.The Nufound to be increased from 9.86 to 17.61 for the hybrid plate while 8.64 to 17.19 for the smooth absorber plate corresponding to Reranges.Although the ffound to be higher for hybrid (0.228–0.088) than smooth plate (0.153–0.060) but the overall THPP remained superior from hybrid plate. So, the results depicts that the proposed hybrid roughened absorber plate is an effective heat transfer enhancement technique in SAH.

Keywords: Artificial roughness,Computational fluid dynamics,Hybrid roughness,Nusselt number,Solar air heater,Thermo-hydraulic performance

1. Introduction

Solar air heaters (SAHs) are among the extensively used solar thermal devices because of their simple structure, low operating cost, ease of maintenance, and suitability for applications in industrial thermal systems[1]. Despiteof these advantages, the thermal efficiency of conventional SAH remains relatively low due to the poor convective heat transfer coefficient between the absorber plate and the flowing air. The laminar sublayer next to the heated absorber surface creates significant thermal resistance, limiting the rate of heat transfer from the absorber plate to the air stream [2], [3].

Researchers have focused on variety of techniques including fins, baffles, vortex generators, wire ribs, and artificial roughness elements to improve thermal performance. Among these techniques, artificial roughness has emerged as one of the most effective methods because it enhances heat transfer without requiring external power input [4], [5]. Artificial roughness elements disturb the hydrodynamic and thermal boundary layers, generate localized turbulence, and promote momentum exchange between the wall-adjacent fluid and the core flow region. Consequently, the convective heat transfer coefficient and thermal efficiency of the SAH are significantly improved [6].

Over the past two decades, researchers have focused on investigating variety of roughness geometries including transverse ribs, inclined ribs, V-shaped ribs, multi-V ribs, arc-shaped ribs, wedge-shaped ribs, and dimpled surfaces. It was observed that experimental plus numerical investigations have been inspected for enrichment in the Nusselt number as compared to smooth duct[7], [8]. However, the increase in heat transfer is generally go together with by an increase in f and pressure drop, which leads to additional pumping power requirements. Therefore, the design of an effective roughness geometry requires a cautious balance between thermal improvement and hydraulic penalty.

Among the various rib geometries investigated in literature, V-shaped ribs found to get the attention of researchers as they generate strong secondary flow structures and improve fluid mixing near the absorber surface. The converging and diverging flow developed by the V-shaped ribs promotes enhanced turbulence generation and boundary-layer disruption. This results in higher heat transfer rates than conventional transverse ribs [2], [9]. In recent times, researchers have been focusing on advanced roughness concepts which demonstrate the superior thermo-hydraulic performance. It has been observed that Hybrid roughness geometries depictthe promising results [10], [11].

Computational Fluid Dynamics (CFD) has become a powerful tool for investigating the complex flow and heat transfer phenomena occurring inside roughened SAH ducts. CFD allows the researchers to visualize the of complex flow mechanisms associated in hybrid SAH that are difficult to obtain experimentally. The advanced turbulence models like SST k–ω allowed the researchers in predicting near-wall turbulence behavior, flow separation, and heat transfer enhancement in roughened ducts [12], [13]. Consequently, CFD has been become extensively explored tool to investigate the roughness geometries and evaluate their thermo-hydraulic performance under various operating conditions.

From literature, it has been observed that majority of studies investigated individual roughness geometries, so comparatively limited research papers reflected in literature focused on hybrid roughness plate. A comprehensive understanding of the hybrid plate is essential for developing high-performance SAH systems.

The goal of the present study is to comparative investigation of the smooth and hybrid SAH plate using CFD. The investigation focused on evaluation of flow behavior, thermal behavior, pressure behavior, and THPP of the both the plates under identical conditions.

The outcomes of this present study are likely to provide useful design guidelines for the development high-performance SAH.

2. Methodology

2.1 CFD Domain and Geometry

A three-dimensional SAH duct was modeled and analyzed using CFD to investigate the THPP of a hybrid roughened absorber plate. The geometry consisted of an inlet section, a heated test section, and an outlet section to ensure fully developed flow conditions within the test region. Two configurations were considered in the present study, namely a conventional smooth duct and a hybrid roughened duct.

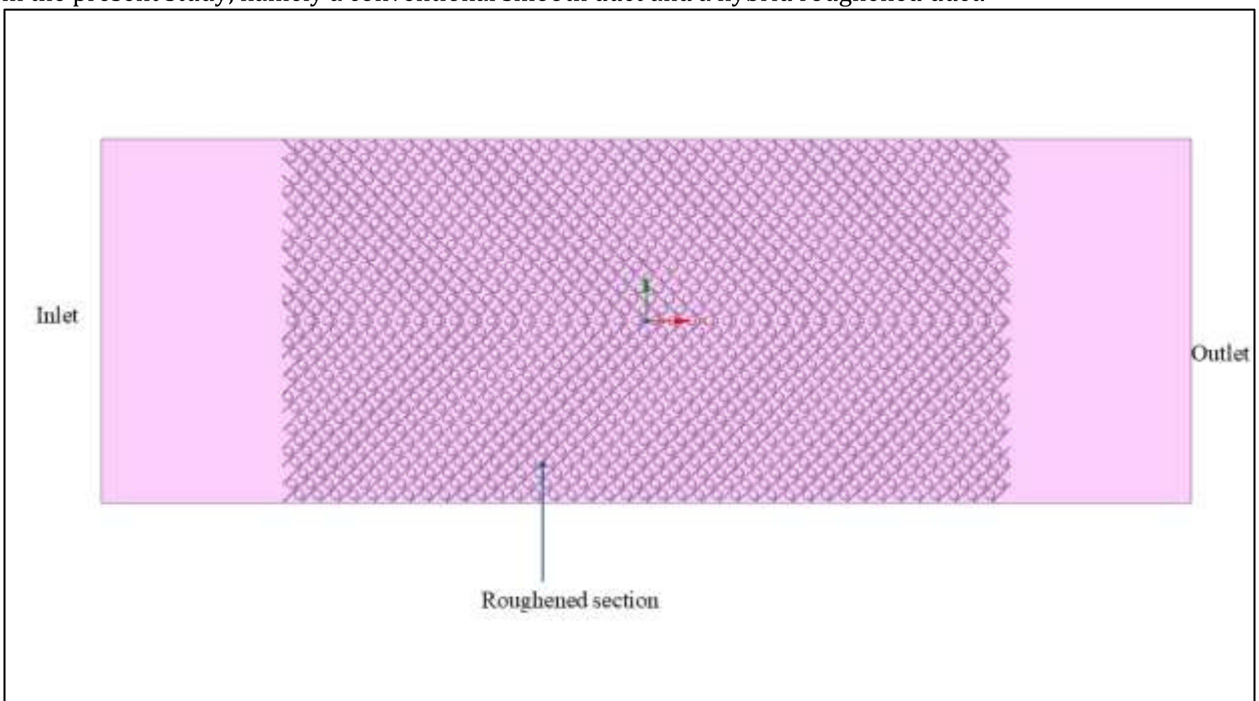

Figure 1 The hybrid roughness configuration

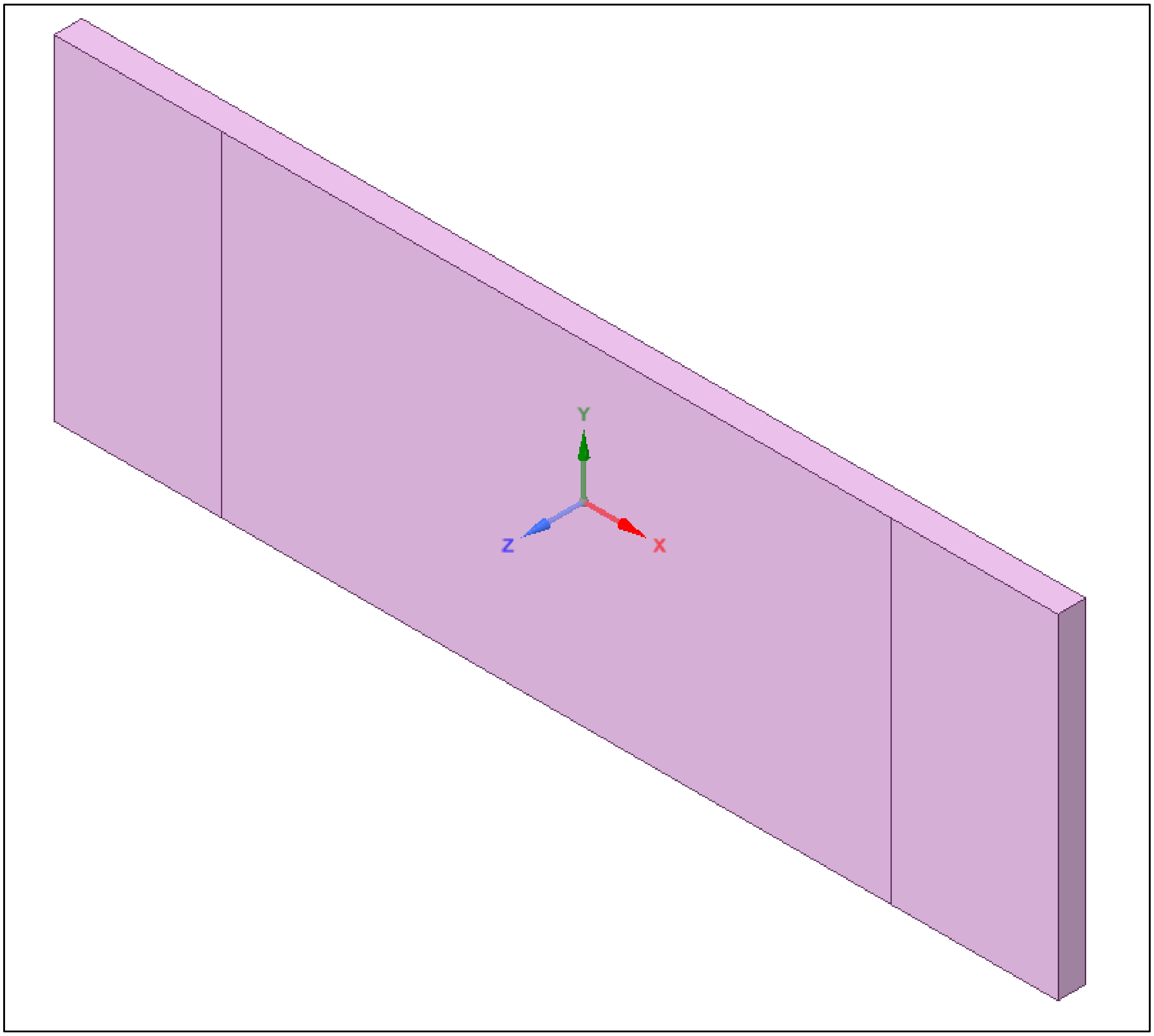

Figure 2 The smooth plate configuration

The hybrid roughened plate comprised V-shaped ribs + dimple elements mounted on the absorber surface. The geometrical dimensions of the duct and roughness elements were selected based on the optimum parameter ranges reported in previous investigations on artificially roughened SAHs[6], [7], [14]. The geometric parameters are given in Table 1.

Table 1 The parameters used to create geometries in the present study

Parameter	Symbol	Value	Unit
Duct width	W	300	mm
Duct height	H	25	mm
Inlet length	Li	150	mm
Test section length	Lt	600	mm
Outlet length	Le	150	mm
Total duct length	L	900	mm
Hydraulic diameter	Dh	46.15	mm
Rib height	e	1.5	mm
Relative roughness height	e/Dh	0.032	–

Rib pitch ratio	P/e	10	–
Rib pitch	P	15	mm
Rib width	w	1	mm
Rib inclination angle	α	60	°
Total duct length	L	900	mm
Hydraulic diameter	Dh	46.15	mm
Rib height	e	1.5	mm
Wall clearance	C	24	mm
Dimple diameter	D	8	mm
Dimple depth	d	1.6	mm
Relative dimple depth	d/Dh	0.035	–
Streamwise dimple pitch	Sl	15	mm
Transverse dimple pitch	St	9	mm
Pitch ratio	St/Sl	0.60	–
Gap between rib apex and dimple	g	2	mm

2.2 Meshing and Grid testing

The three-dimensional geometries of smooth and hybrid have been meshed using ANSYS 2024R1.Inflation layers were generated adjacent to the absorber surface to improve near-wall resolution and accurately predict viscous sublayer behavior.

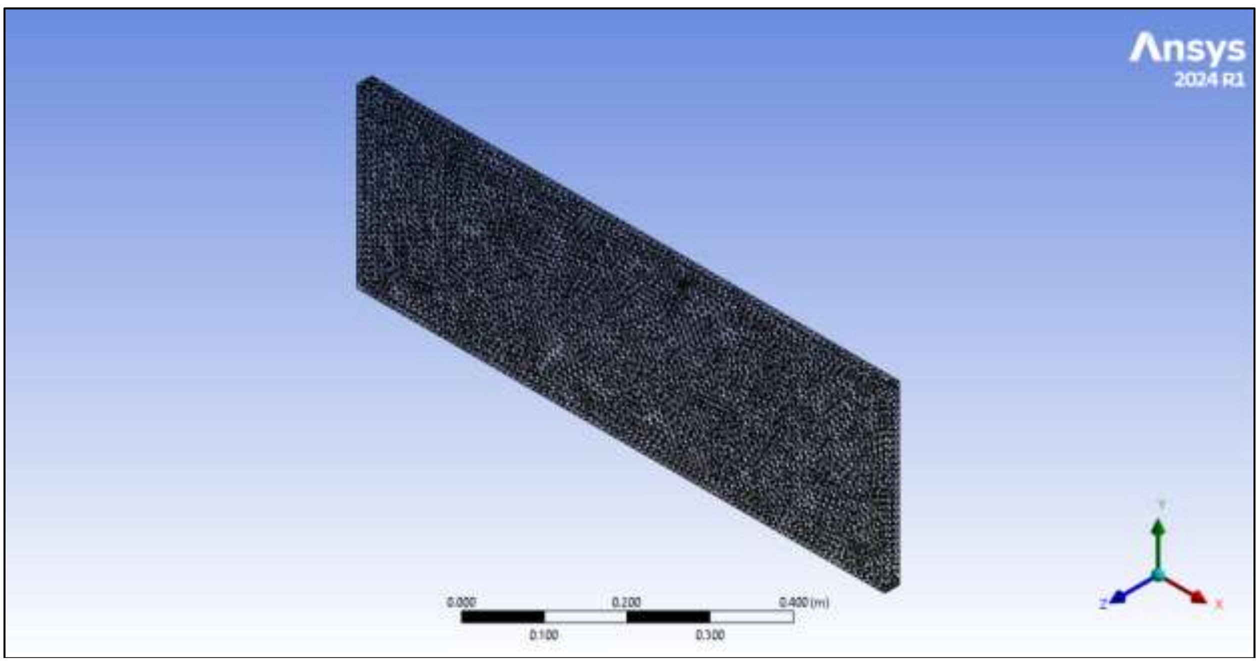

Figure 3 Meshing of the smooth plate configuration

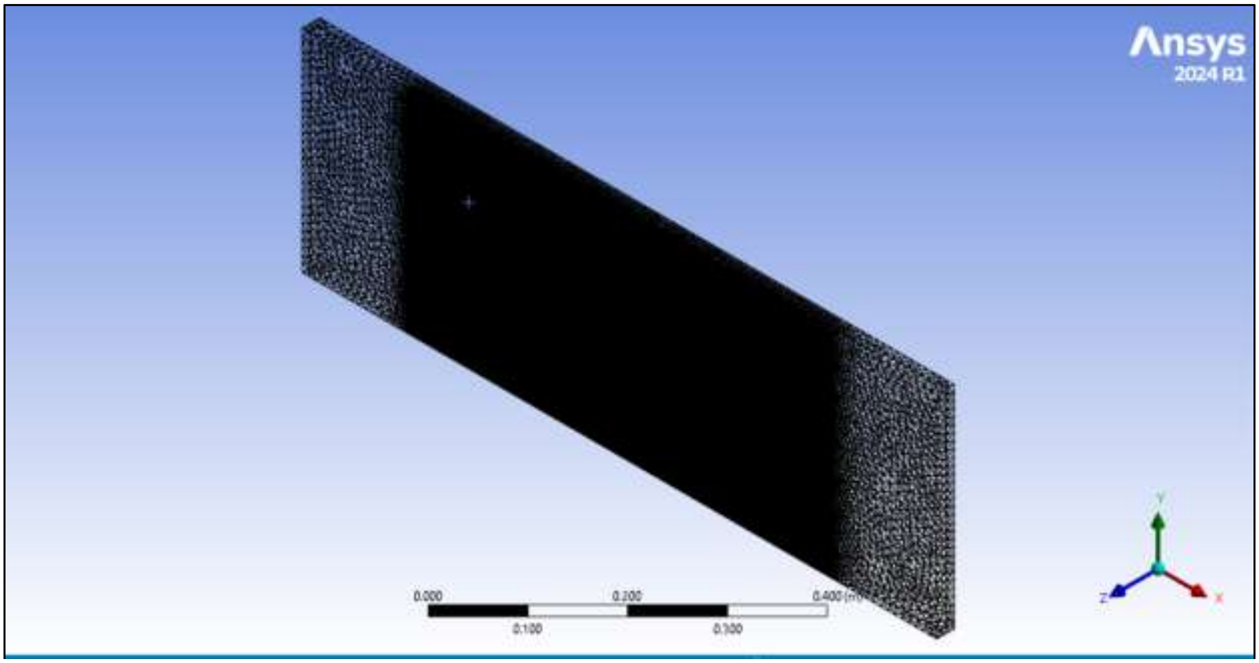

Figure 4 Meshing of the hybrid roughness configuration

Similar types of meshing approaches have already been successfully adopted in recent CFD investigations of roughened SAH ducts [11], [12].
The grid independence test has been applied for three different element sizes corresponding to coarse, medium, and fine meshes. In this process, the outlet temperature (mass-weighted) has been monitored as it reflects the heat transfer characteristics of the SAH. This test indicates that's the mesh is independent of mesh size.
Therefore, the medium mesh size was adopted for meshing the geometries of absorber plates

2.3 Governing Equations

The CFD simulation has been performed under steady-state turbulent flow conditions. The conservation of mass, momentum, and energy equations have been solved in CFD simulation.These equations have been widely applied in CFD studies involving turbulent flow and heat transfer [1]
The continuity equation is expressed as:

$$\nabla \cdot \left(\rho\vec{V}\right) = 0$$

The momentum equation is given by:

$$\nabla \cdot (\rho\vec{V}\vec{V}) = -\nabla P + \nabla \cdot (\mu\nabla\vec{V})$$

The energy equation can be written as:

$$\nabla \cdot \left(\rho\vec{V}T\right) = \nabla \cdot (k\nabla T)$$

2.4 Turbulence Model

In our investigation, SST k–ω turbulence model has been applied. Theapplied model combines the advantages of the standard k–ω formulation in the near-wall region with the robustness of the k–ε model in the free-stream region through a blending function [13].
Previous CFD studies on roughened SAH have reported that the appliedmodel provides superior prediction of flow and heat transfer characteristics compared with conventional two-equation turbulence models [11], [12]. Therefore, the adoptedmodel because of its proven capability in predicting turbulence interaction.

2.5 Boundary Conditions

The CFD simulations have been performed using the pressure-based solver in ANSYS Fluent under steady-state conditions. The air has been used as the working fluid, and its thermophysical properties have been assumed as constant throughout the analysis.

The inlet velocities ranging from 0.5 to 2.0 m/s while the inlet air temperature was maintained at 300 K. A uniform heat flux of 1000 W/m² was applied to the absorber surface. Similar thermal conditions have been widely adopted in CFD investigations of SAH ducts [2], [11].The outlet boundary was defined as a pressure outlet, while all walls were subjected to the no-slip condition. The remaining duct walls were assumed adiabatic.

2.7 Validation of Numerical Model

The numerical model was validated using established empirical correlations for smooth duct flow. The Nu predicted by the CFD model was compared with the Dittus–Boelter correlation, whereas the f was compared with the Blasius correlation for turbulent flow in smooth ducts [12].

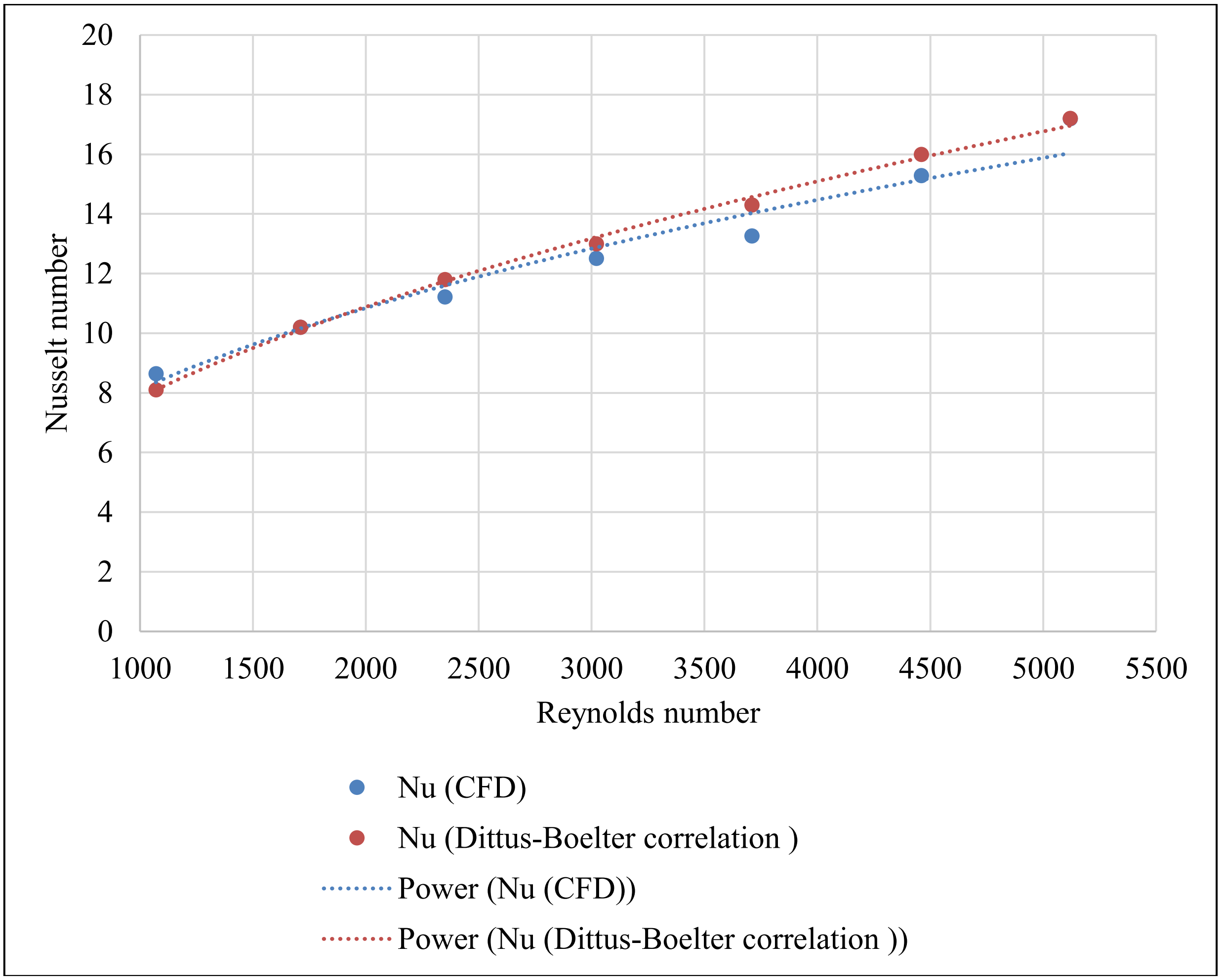

Figure 5Comparison of CFD-predicted Nu with the Dittus–Boelter correlation for the smooth SAH duct.

Figures 5 and 6 compare the CFD-predicted Nu and f with the Dittus–Boelter and Blasius correlations, respectively. Good agreement was observed between the numerical and theoretical results, with maximum deviations of 7.26% for the Nu and 2.89% for the f. These deviations are within acceptable limits reported in previous CFD investigations of SAHs, confirming the reliability of the adopted numerical methodology.

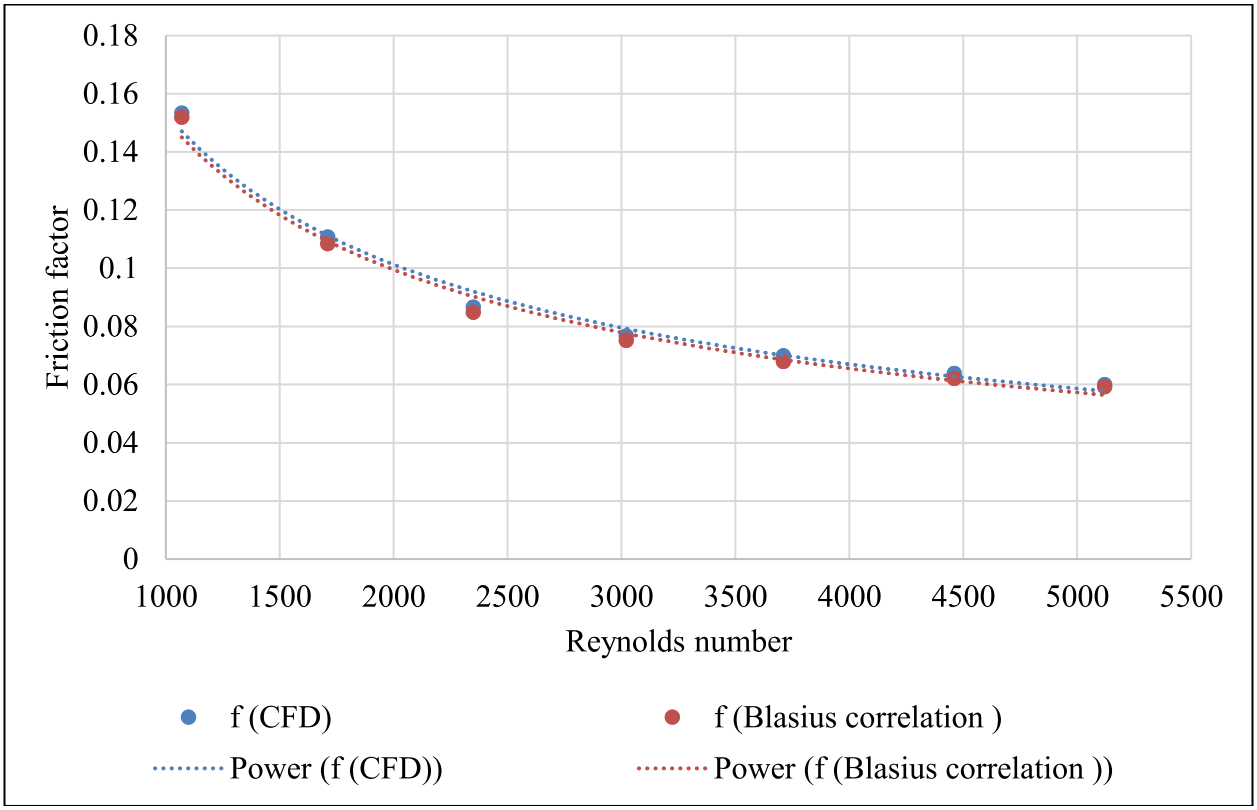

Figure 6 Comparison of CFD-predicted f with the Blasius correlation for the smooth SAH duct.

The CFD predictions exhibited satisfactory agreement with the theoretical correlations, with deviations remaining within acceptable limits reported in previous SAH investigations[7], [15]. The observed trends of increasing Nu and decreasing f with Refurther confirmed the reliability and accuracy of the adopted numerical methodology.

The validation results demonstrate that the selected mesh strategy, boundary conditions, and SST k–ω turbulence model is capable of accurately predicting the THPP characteristics of SAH ducts.

3. Results and Discussion

3.1 Flow Field Characteristics

The flow characteristics inside the SAH duct have been analyzed using velocity contours and streamline distributions to explore the influence of the hybrid roughness geometry in SAH. The comparison between the smooth and hybrid roughened ducts has been performed at an inlet velocity ranging from 0.5-2 m/s, corresponding to the Re investigated in the present study.

3.1.1 Comparative Analysis of Velocity Magnitude Contours

Figures 7 and Figures 8 the comparison of velocity magnitude contours of the smooth and hybrid roughened absorber plates has been presented.It has been observed that the smooth plateshows uniform velocity distribution throughout the duct. The highest velocities concentrated in the core flow region and a gradual reduction in velocity toward the duct walls due to the no-slip boundary condition. The absence of flow-disturbing elements allows the airflow to develop smoothly. This results in the formation of a stable hydrodynamic boundary layer and limited turbulence generation. Consequently, fluid mixing near the heated absorber surface remains weak which leads to comparatively lower convective heat transfer.

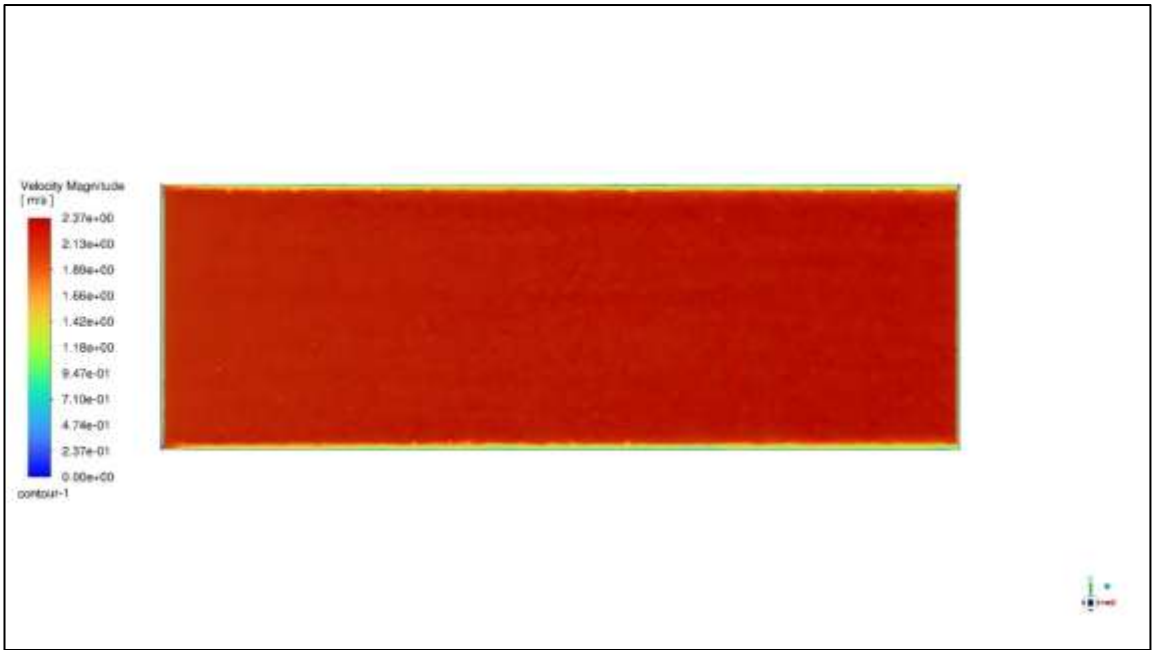

Figure 7Velocity magnitude contour for Smooth SAH duct

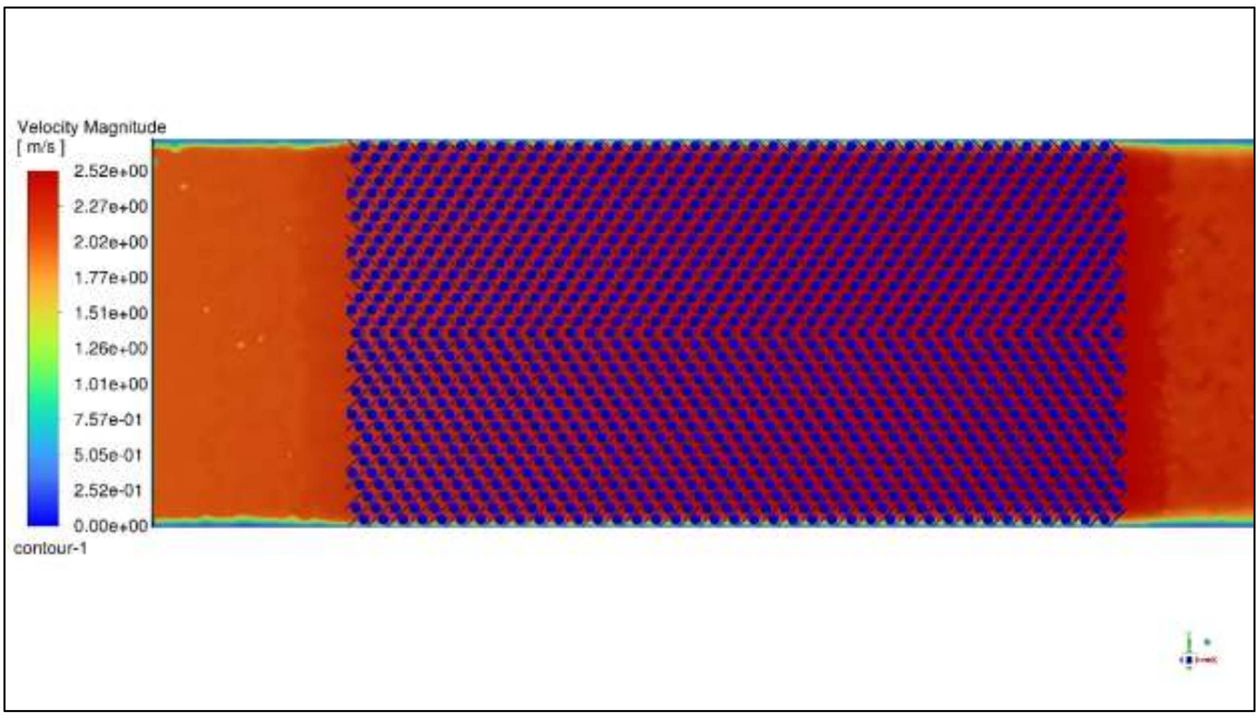

Figure 8 Velocity magnitude contour for hybrid roughenedSAH duct

In the hybrid roughened absorber plate, it has been observed that it significantly modifies the flow structure by presenting repeated disturbances to the boundary layer. As the airflow interacts with the hybrid roughness elements, local acceleration of the fluid occurs around the roughened regions, increasing the peak velocity from approximately 2.37 m s^{-1} in the smooth duct to 2.52 m s^{-1} in the hybrid duct. The repeated flow separation and reattachment generated by the roughened plate produce secondary vortices and localized recirculation zones. This results in a more heterogeneous velocity field than that observed in the smooth configuration.

The enhanced turbulence zone created by the hybrid roughened plate promotes continuous momentum exchange between fluid particles. This intensified mixing disrupts the thermal boundary layer which enablesthe cooler air to reach the heated surface more effectively which ultimately increase the convective heat transfer coefficient. So, it has been inferred the hybrid absorber plate exhibits a higher Nusselt number and improved thermal efficiency compared with the smooth absorber plate.

Therefore, the comparative velocity contours depicts that the hybrid absorber plate provides a more effective heat transfer enhancement than the smooth absorber plate.

Overall, the velocity contour demonstrates that the hybrid roughness configuration effectively promotes boundary-layer disruption, turbulence generation, and secondary flow interaction, improved THPP compared with a smooth SAH duct.Similar flow behavior has been reported by [15], [16], and[1], who observed enhanced turbulence generation and boundary-layer disruption in roughened SAH ducts.

3.2 Pressure Distribution Analysis

3.2.1 Comparative Analysis of Static Pressure Contours

The static pressure contours for the smooth and hybrid roughened absorber plates are shown in Figures 11 and Figure 12, respectively. The pressure distributions depict the influence of artificial roughness on the hydraulic characteristics of the SAH duct. It has been observed that the pressure decreases gradually and almost linearly from the inlet to the outlet in the case of smooth absorber plate. This indicates the stable fully developed turbulent flow with relatively low hydraulic resistance. Since no flow-obstructing roughness elements are present, the airflow experiences minimal momentum loss, resulting in a comparatively low pressure drop across the duct.

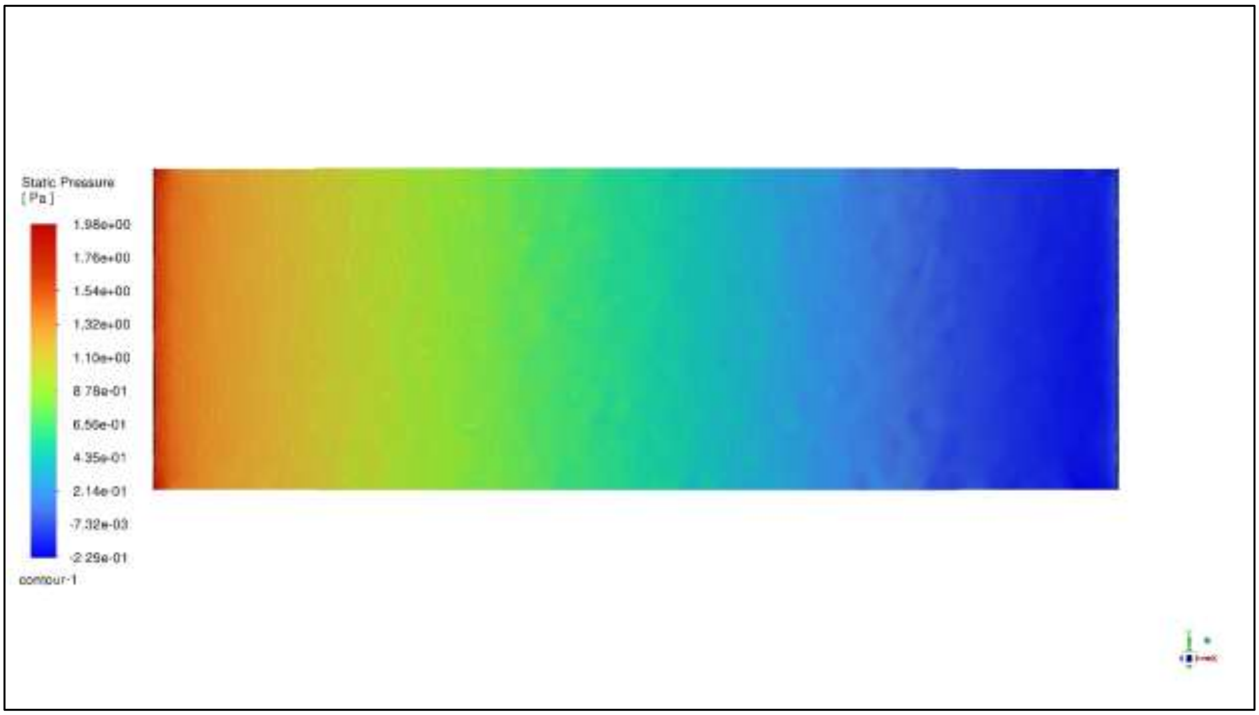

Figure 9the static pressure contour for the smooth SAH duct

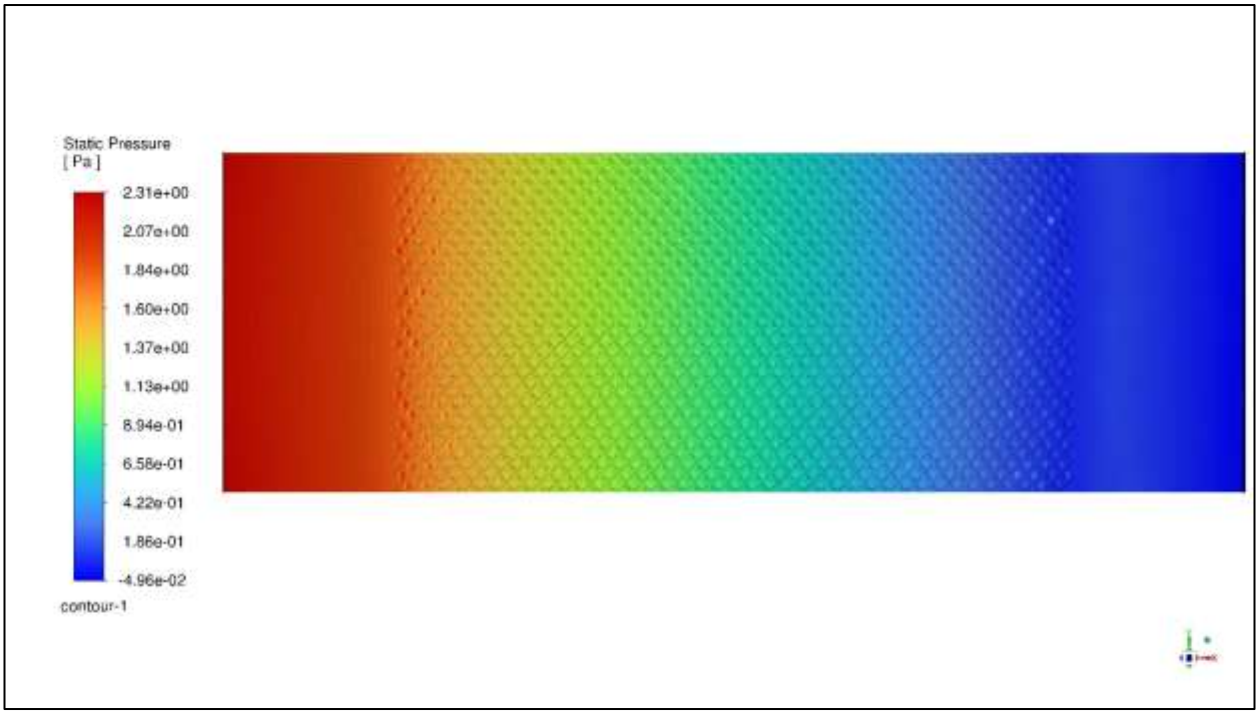

Figure 10the static pressure contour for the hybrid roughened SAH duct

In case of the hybrid roughened absorber plat, it exhibits a more complex pressure distribution due to the presence of the roughness elements.

As the air passing over the roughness elements the high-pressure regions are formed on the upstream faces of the ribs and dimples, while low-pressure regions develop immediately downstream because of flow separation and wake formation.

These repeated pressure fluctuations indicate continuous acceleration and deceleration of the airflow as it passes over the roughened surface. It has been observed that he interaction between the fluid and the hybrid roughness enhances momentum exchange and turbulence generation, but it also increases the overall hydraulic resistance within the duct.

Further, the hybrid configuration experienced the steeper pressure gradient as compared with the smooth absorber plate, along the flow direction. The inlet pressure has increased from approximately 1.98 Pa for the smooth duct to 2.31 Pa for the hybrid duct. It indicates that additional pressure is required to overcome the resistance induced by the roughness elements. The repeated obstruction of the flow by the hybrid ribs increases form drag in addition to viscous shear losses, resulting in a greater overall pressure drop. This behavior is a direct consequence of the intensified turbulence, repeated flow separation and reattachment, and secondary flow structures generated by the hybrid roughness.

The increased pressure gradient has been observed across the hybrid plate section is a consequence of additional form drag and momentum dissipation generated by the roughness elements. Similar observations have been reported by [17], [18]

Overall, the smooth absorber plate demonstrates a stable pressure in the duct with minimal resistance and lower pumping power requirements but have limited heat transfer capability. The observed pressure distributions confirm that the hybrid roughness effectively enhances the THPP of the SAH despite the associated increase in pressure drop.

3.3 Thermal Characteristics

3.3.1Comparative Analysis of Temperature Contours

Figures 13 and Figure 14 present the static temperature contours for the smooth and hybrid roughened absorber plates, respectively.

In the smooth absorber plate, the air enters the duct at 300 K and experiences a gradual temperature increase along the flow direction as heat is transferred from the heated absorber surface.

The temperature shows a relatively smooth and continuous gradient from the inlet to the outlet, demonstrating limited turbulence and weak convective mixing.

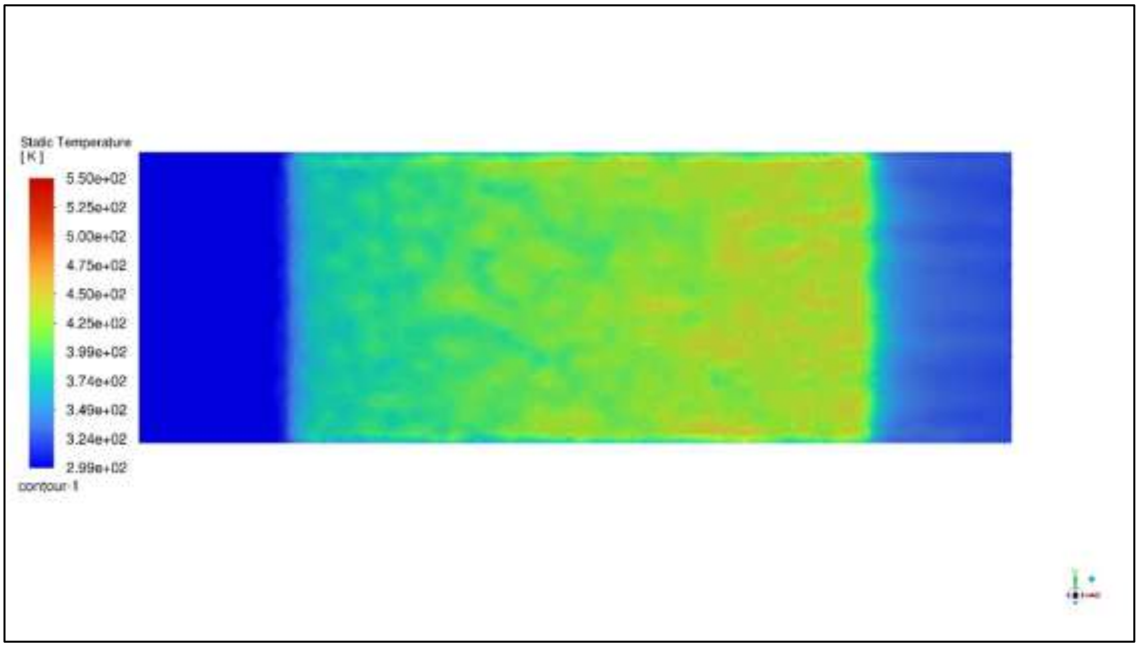

Figure 11 The Static temperature contour for the smooth SAH duct

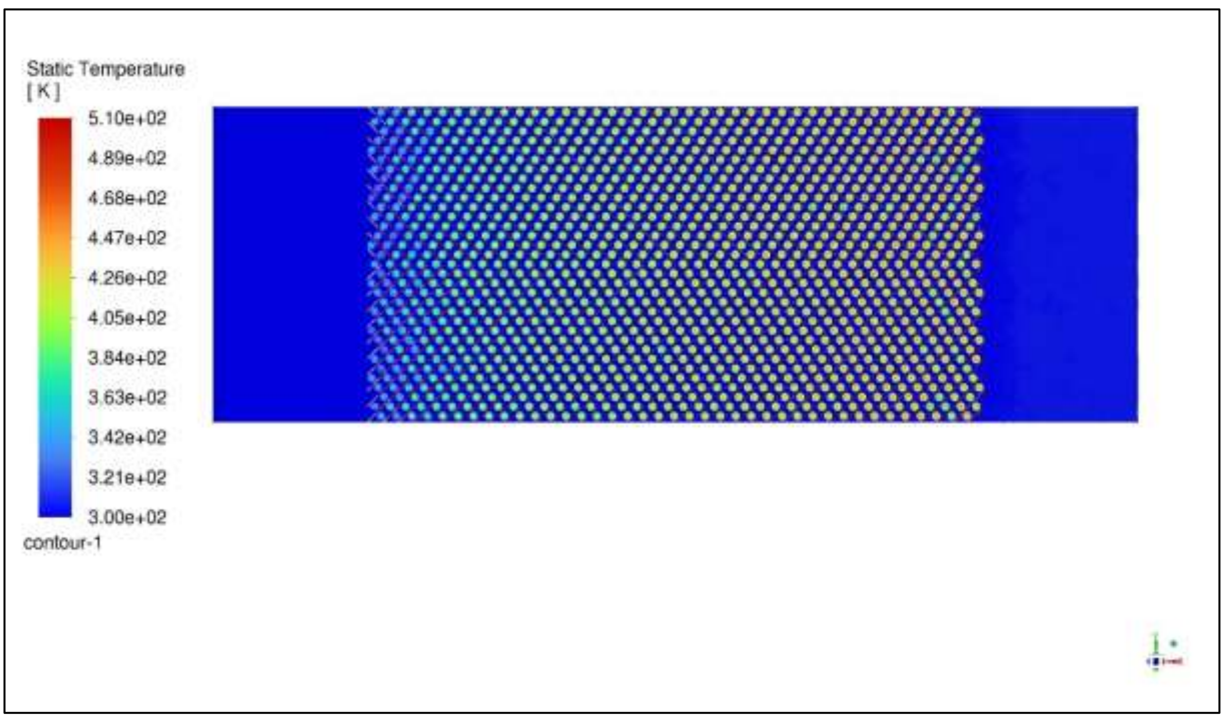

Figure 12 The Static temperature contour for the roughened SAH duct

In the case of hybrid roughened absorber plate, it shows a significantly different temperature distribution as compared to baseline. The presence of hybrid roughness elements interrupts the thermal boundary layer and promotes repeated flow separation, and reattachment.

Subsequently, a much larger portion of the airflow is exposed to elevated temperatures, as evidenced by the contours. These temperature variations depict more effective transfer of thermal energy from the absorber plate to the flowing air compared with the smooth plate.
As a result, the hybrid absorber plate produces a more uniform temperature across the duct cross-section and attains a higher outlet air temperature than the smooth absorber plate.
Further, it was observed from the temperature contour that it indicates effective thermal mixing and continuous disruption of the thermal boundary layer within the roughened section. This behavior is in line with the observations of[19]. Similar conclusions were identified by[17], the findings depict that absorber geometry as one of the most influential parameters governing thermal performance in SAH
Overall, the findings are demonstrating the superiority of the hybrid roughened absorber plate for high-performance SAH

3.4 Thermo-Hydraulic Performance

3.4.1 Comparative Analysis of Nusselt Number

The variation of Nu with Re for smooth and hybrid plate can be observed in Figure 15.
It has been observed that Nu increases continuously with increasing Re for both plates. As the Re increases from approximately 1100 to 5100, the Nusselt number of the smooth plate varies from 8.64 to 17.19, whereas the hybrid plate varies from 9.86 to 17.61.

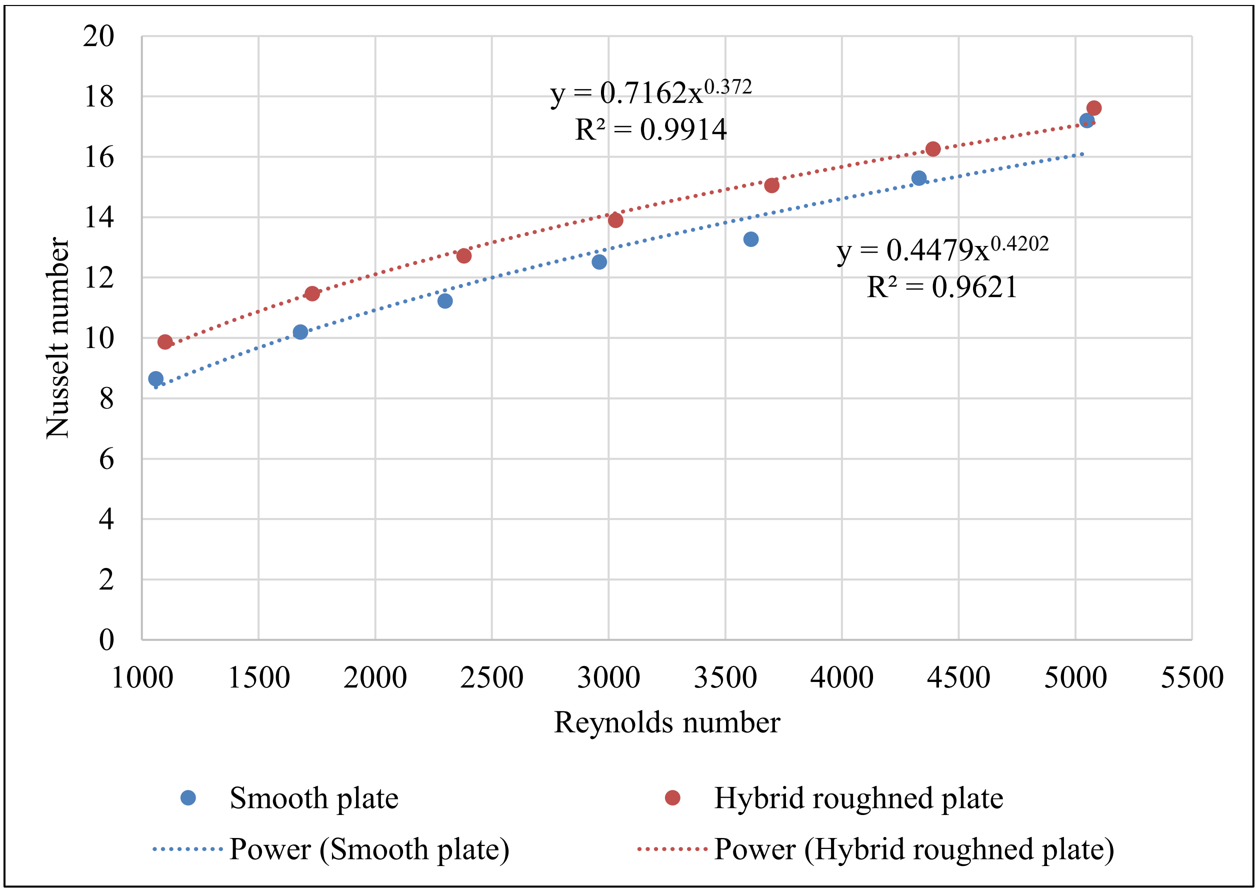

Figure 13 variation of Nu with Re for the smooth and hybrid roughened SAH duct

It has been identified that the hybrid absorber plate produces higher Nusselt numbers than the smooth absorber plate.
These flow structures enhance turbulence intensity and promote efficient mixing between the high-energy core flow and the fluid adjacent to the heated absorber surface, thereby increasing the convective heat transfer coefficient. Similar observations have been reported by [5], [6], [8], [20], [21], [22]who demonstrated that

artificial roughness substantially improves heat transfer by continuously disturbing the thermal boundary layer.
The smooth absorber plate follows the correlation $Nu = 0.4479\ Re^{0.4202}$, $R^2 = 0.9621$, whereas the hybrid roughened absorber plate is represented by $Nu = 0.7162\ Re^{0.372}$, $R^2 = 0.9914$. The higher R^2 value obtained for the hybrid configuration indicates a stronger correlation between the numerical data and the proposed model. It suggests that the heat transfer behavior is determined with high accuracy over the investigated Re range.
Although both configurations display similar increasing trends, the enhancement achieved with the hybrid roughness remains consistently indicating its superior heat transfer capability. This enhancement agrees well with previous investigations, which reported that optimized rib and hybrid roughness geometries significantly increase the convective heat transfer coefficient while maintaining acceptable hydraulic penalties [8], [15], [21], [22].
Overall, the hybrid roughened absorber plate shows superior thermo-hydraulic characteristics compared with the conventional smooth absorber plate, making it a promising design for SAH.

3.4.2 Friction Factor Analysis

Figure 16 presents the variation of the friction factor with Re for the smooth and hybrid roughened absorber plates.

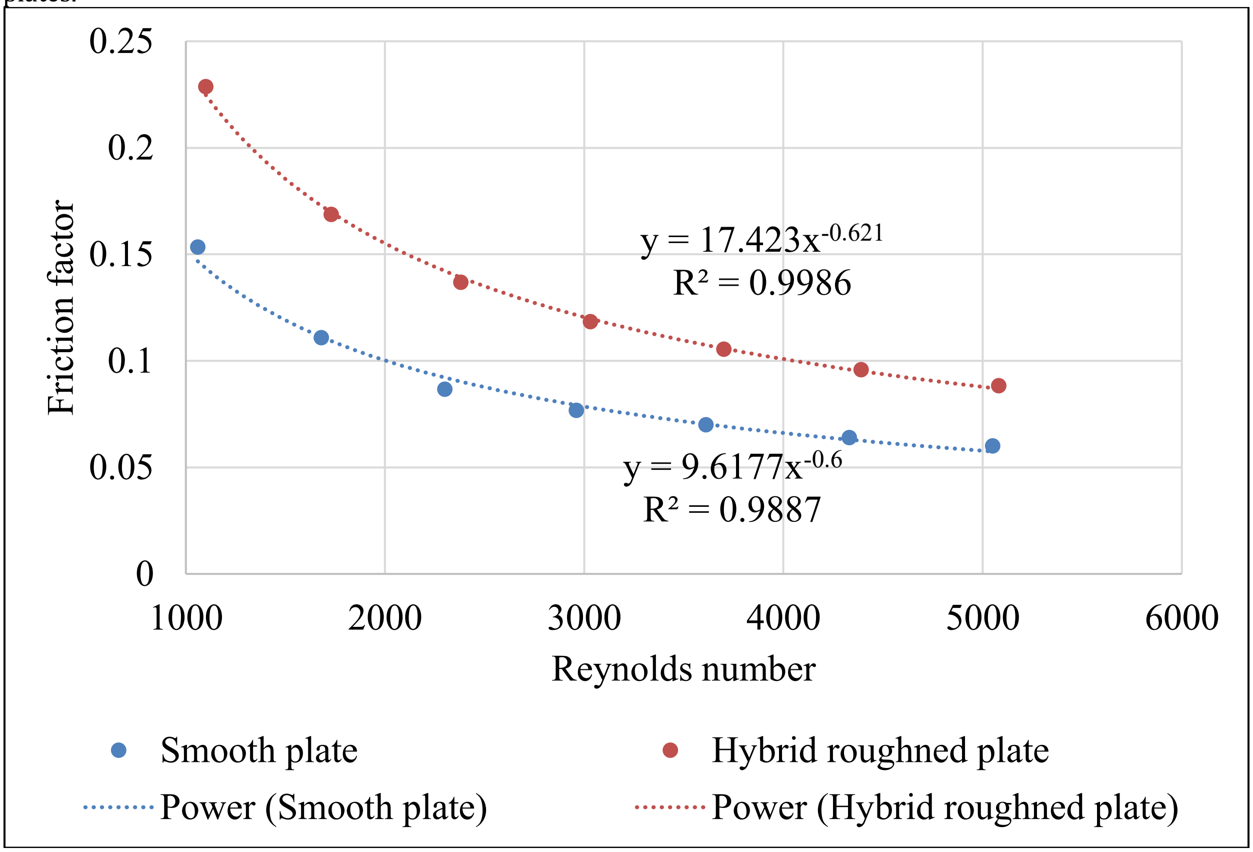

Figure 14 variation of f with Re for the hybrid roughened SAH duct

The variation of f with Recan be observed in fig. 16. The variation indicates that the friction factor decreases with increasing Re for both plates, which agrees with the characteristics of turbulent flow in internal ducts. It has been observed that as Reynold number increases, the friction value follows the downtrend. The f of smooth plate comes down to 0.060 from 0.153 while it drops to 0.088 from 0.228 for the hybrid roughened absorber plate
This happens because of the increased dominance of inertial forces over viscous forces, resulting in relatively lower wall friction at higher flow velocities[8].
It has been found that the hybrid roughened absorber plate consistently displays a higher friction factor than the smooth absorber plate over the entire Re range.

Similar behavior has been reported by[6], [8], [15], [23]. These studies have confirmed that artificial roughness improves turbulence generation but concurrently increases frictional losses.

The regression analysis reveals a strong correlation between the friction factor and Re for both the absorber plates. The smooth absorber plate follows the correlation $f = 9.6177\ Re^{-0.6}$with a coefficient of determination of $R^2 = 0.9887$, while the hybrid roughened absorber plate is represented by $f = 17.423\ Re^{-0.621}$ with an excellent coefficient of determination of $R^2 = 0.9986$. The values of R^2 indicate that the proposed correlations accurately describe the variation of friction factor over the investigated Rerange and can be used for engineering predictions within the studied operating conditions.

The comparison reveals that the hybrid roughened absorber plate shows an average friction factor approximately 45–50% higher than that of the smooth absorber plate. This indicates that the hydraulic penalty is related with the introduction of artificial roughness.

From observation of results, it has been observed that hybrid roughness significantly improved heat transfer. Similar observations have been reported by[5], [21], [22], [24]. It was concluded thar who concluded that, enhancement in convective heat transfer generally outweighs the additional pumping power requirement.

3.5 Thermo-Hydraulic Performance Analysis

The THPP was employed to evaluate the overall effectiveness of the hybrid roughness configuration by simultaneously considering heat transfer enhancement and frictional losses. The THPP was calculated using:

$$THPP = \frac{\frac{Nu_r}{Nu_s}}{\frac{f_r}{f_s}^{1/3}}$$

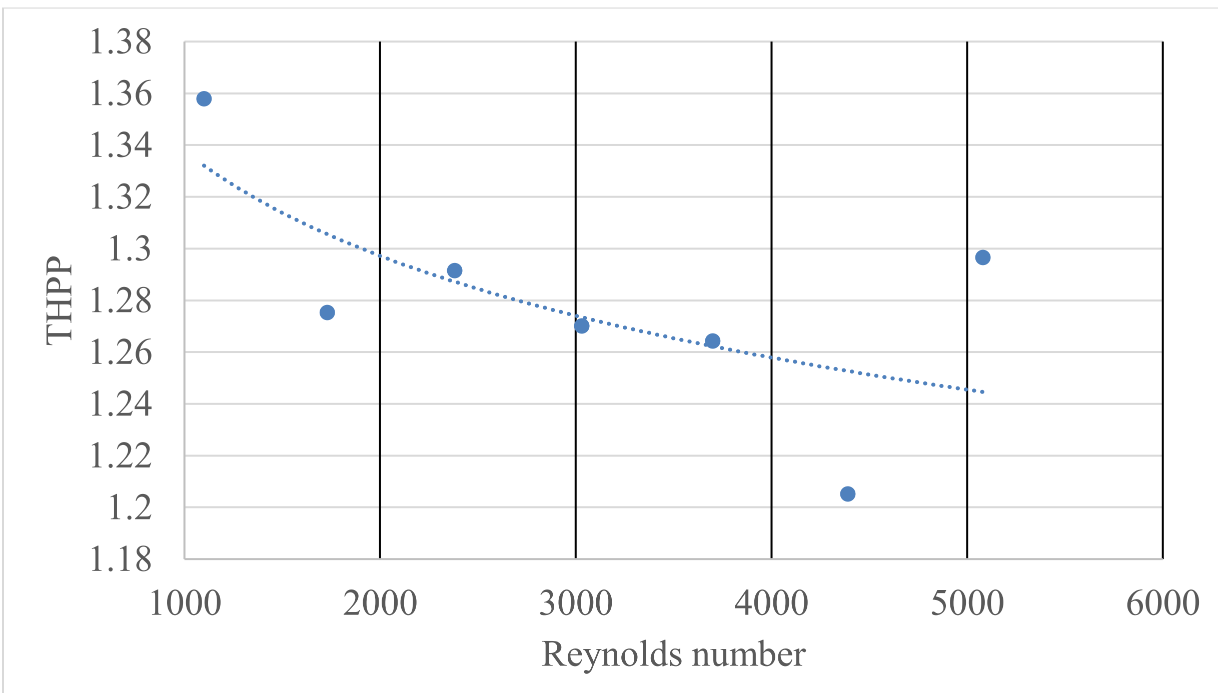

Figure 15 Variation of the THPP of the hybrid roughened absorber plate with *Re*

Figure 17 illustrates the variation of the THPP of the hybrid roughened absorber plate withRe. The THPP is a widely accepted performance criterion that simultaneously evaluates the enhancement in heat transfer and the associated increase in frictional losses. The THPP is a widely accepted criterion for evaluating the combined THPP of roughened SAHs under constant pumping power conditions. A THPP value greater than unity indicates that the enhancement in convective heat transfer outweighs the corresponding increase in friction losses, thereby confirming the effectiveness of the proposed roughness geometry [25], [26].

As shown in Figure 17, the THPP of the hybrid roughened absorber plate remains greater than 1.20 over the entire investigated Rerange, confirming that the hybrid roughness provides a net improvement in the overall

THPP of the SAH. The maximum THPP of approximately 1.36 is observed at a Reof around 1100, indicating that the hybrid roughness is particularly effective under low-flow conditions where enhanced turbulence generation significantly improves heat transfer. As the Reincreases, the THPP gradually decreases to approximately 1.26 around 3700, followed by a slight recovery at the highest Reinvestigated. This behaviour suggests that although the frictional losses increase with increasing flow velocity, the enhancement in convective heat transfer continues to compensate for the additional hydraulic resistance.

The relatively higher THPP at lower Reis attributed to the efficient disruption of the thermal boundary layer by the hybrid roughness elements. The repeated flow separation, reattachment, and secondary vortex formation promote strong fluid mixing near the heated absorber surface, thereby increasing the Nusselt number more rapidly than the corresponding increase in friction factor. At higher Re, the natural turbulence of the flow becomes more dominant, reducing the relative contribution of the roughness-induced turbulence and resulting in a gradual decrease in THPP. Similar trends have been reported by[8], [15], [22], [23] who observed that artificially roughened SAHs generally exhibit their highest thermo-hydraulic performance within the low to moderate Rerange.

Despite the slight reduction in THPP with increasingRe, all experimental points remain well above unity, confirming that the thermal enhancement provided by the hybrid roughness consistently outweighs the associated frictional losses. The trendline also indicates a relatively stable thermo-hydraulic behavior across the investigated operating conditions, suggesting that the hybrid roughness maintains its effectiveness over a wide range of flow rates.

Overall, the THPP results demonstrate that the hybrid roughened absorber plate successfully balances heat transfer enhancement and hydraulic performance. The consistently high THPP values confirm that the proposed hybrid roughness effectively improves the overall efficiency of the SAH and represents a promising passive heat transfer enhancement technique for practical solar thermal applications.

3.5 Limitations of the Study

Although the present CFD investigation provides valuable insights into the THPP of smooth and hybrid roughened absorber plates, some limitations should be recognized. First, the study is based exclusively on numerical simulations, and experimental validation of the proposed hybrid roughness geometry was not performed. While the numerical model was validated against established correlations reported in the literature, experimental verification would further enhance the reliability of the findings.

Second, the simulations were conducted under steady-state conditions with a uniform heat flux applied to the absorber plate. In practical SAH systems, solar radiation intensity varies with time and environmental conditions, resulting in transient operating behavior that was not considered in the present study.

Third, the analysis was restricted to a specific hybrid roughness configuration consisting of V-shaped ribs integrated with dimple elements. Other geometric parameters, such as rib angle, rib height, dimple diameter, pitch ratio, and roughness arrangement, were not optimized. Therefore, the reported results are applicable only to the investigated geometry and operating conditions.

Finally, the study considered a Rerange of 1100–5100 using air as the working fluid. The performance of the proposed roughness under higher Re, different working fluids, or varying thermal boundary conditions remains to be investigated.

3.6 Practical Implications of the Study

The findings of this study depicts that hybrid roughness significantly enhances THPP of SAHas compared to smooth absorber plates.

The detailed CFD analysis of absorber plates offers valuable insights into the flow and heat transfer mechanisms associated with hybrid roughness. It could help the engineers and designers in selecting suitable roughness configurations for high-performance SAH.

The superior THPP observed in the present investigation suggests that hybrid roughened absorber plates have considerable potential for practical applications such as agricultural crop drying, food processing, timber seasoning, industrial drying, space heating, and solar-assisted ventilation systems.

3.7 Future Scope

- Experimental validation of the proposed hybrid roughness under outdoor operating conditions.
- Multi-objective optimization of rib and dimple geometric parameters using optimization algorithms.
- Investigation of transient solar radiation and varying climatic conditions.

• Evaluation of different turbulence models, including LES and DES, for improved prediction of complex flow structures.
• Extension of the numerical methodology to other hybrid roughness configurations and wider Reranges.
• Exergy, entropy generation, and economic analyses to assess the overall performance and practical feasibility of hybrid roughened SAHs.

4. Conclusions

A three-dimensional CFD-based comparative investigation was conducted for smooth and hybrid roughened absorber plates in a SAH under identical operating conditions. The CFD analysis performed using turbulence model, provided detailed insights into the flow behavior, heat transfer characteristics, and hydraulic performance over a Rerange of 1100–5100. Based on the CFD results, the following conclusions can be drawn:
1. It has been found that the hybrid roughened absorber plate significantly modified the flow field by promoting repeated flow separation, reattachment, and localized vortex formation. These flow structures enhanced turbulence intensity and improved momentum exchange between the core flow and the fluid adjacent to the heated absorber surface compared with the smooth absorber plate.
2. The temperature contours confirmed that the hybrid roughness effectively disrupted the thermal boundary layer which results in uniform temperature distribution throughout the duct. Consequently, the hybrid plate revealed higher outlet air temperatures than the smooth absorber plate.
3. It has been observed thatNu increased with corresponding Reincrease for both the plates. More importantly, the hybrid absorber plate consistently outperformed the smooth absorber plate. The Nuincreases from8.64 to 17.19(hybrid plate), compared with 8.56 to 17.10 (smooth plate). This improvement is ascribed to enhanced turbulence generation and continuous renewal of the thermal boundary layer.
4. The hybrid plate causes the hydraulic resistance to the flow, leading to development of higher friction factors (0.228–0.088) than the smooth absorber plate (0.153–0.060). The increase in friction factor resulted from greater wall shear stress and form drag generated by the hybrid roughness elements.
5. It has been observed that despite the increase in friction losses, the THPP found to be greater than unity (1.20-1.36) throughout the investigated Rerange. The maximum THPP of 1.36 confirms that the enhancement of performance despite associated hydraulic penalty. It validates the effectiveness of the proposed hybrid roughness under constant conditions.

Overall, the comparative investigation confirms that the hybrid roughened absorber plate provides superior thermo-hydraulic performance compared with the conventional smooth absorber plate. The enhanced heat transfer achieved through boundary-layer disruption and improved fluid mixing compensates for the increase in pressure drop, making the hybrid roughness a promising passive heat transfer enhancement technique for high-performance SAHs. Future work may focus on experimental validation of the numerical results and parametric optimization of the hybrid roughness geometry to further improve thermal efficiency while minimizing hydraulic losses.

References

[1] H. Kidane, I. Farkas, and J. Buzás, “Role of computational fluid dynamics in solar air heating: a comprehensive overview of applications, benefits, and future directions,” *Journal of Thermal Analysis and Calorimetry*, vol. 150, no. 12. Springer Science and Business Media B.V., pp. 8861–8877, 2025. doi: 10.1007/s10973-025-14261-1.
[2] V. S. Hans, R. P. Saini, and J. S. Saini, “Heat transfer and friction factor correlations for a solar air heater duct roughened artificially with multiple v-ribs,” *Solar Energy*, vol. 84, no. 6. pp. 898–911, 2010. doi: 10.1016/j.solener.2010.02.004.
[3] B. N. Prasad and J. S. Saini, “Effect of artificial roughness on heat transfer and friction factor in a solar air heater,” *Solar Energy*, vol. 41, no. 6. pp. 555–560, 1988. doi: 10.1016/0038-092X(88)90058-8.
[4] B. Bhushan and R. Singh, “A review on methodology of artificial roughness used in duct of solar air heaters,” *Energy*, vol. 35, no. 1. Elsevier Ltd, pp. 202–212, 2010. doi: 10.1016/j.energy.2009.09.010.
[5] A. Kumar and M.-H. Kim, “CFD Analysis on the Thermal Hydraulic Performance of an SAH Duct with Multi V-Shape Roughened Ribs,” *Energies*, vol. 9, no. 6. MDPI, 2016. doi: 10.3390/en9060415.
[6] A. S. Yadav and J. L. Bhagoria, “A CFD (computational fluid dynamics) based heat transfer and fluid flow analysis of a solar air heater provided with circular transverse wire rib roughness on the absorber plate,” *Energy*, vol. 55. Elsevier Ltd, pp. 1127–1142, 2013. doi: 10.1016/j.energy.2013.03.066.

[7] S. Kumar and R. P. Saini, “CFD based performance analysis of a solar air heater duct provided with artificial roughness,” *Renewable Energy*, vol. 34, no. 5. pp. 1285–1291, 2009. doi: 10.1016/j.renene.2008.09.015.
[8] I. Singh and S. Singh, “A review of artificial roughness geometries employed in solar air heaters,” *Renew. Sustain. Energy Rev.*, vol. 92, pp. 405–425, Sep. 2018, doi: 10.1016/j.rser.2018.04.108.
[9] A. Kumar, A. Layek, and P. K. Mondal, “Heat Transfer Analysis of a Solar Air Heater Roughened with Chamfered Rib and Groove Roughness on the Absorber Plate Using CFD Approach,” *Lecture Notes in Mechanical Engineering*. Springer Science and Business Media Deutschland GmbH, pp. 1373–1384, 2020. doi: 10.1007/978-981-15-0124-1_121.
[10] V. Goel, A. Dwivedi, and A. K. Choudhary, “Parametric optimization of hybrid artificial roughness used in solar air heaters using multiple criteria decision making techniques,” *Proceedings of the Institution of Mechanical Engineers, Part A: Journal of Power and Energy*, vol. 237, no. 8. SAGE Publications Ltd, pp. 1823–1841, 2023. doi: 10.1177/09576509231183037.
[11] S. L. Sharma, K. Kishor, V. S. Bisht, A. Debbarma, and A. Gaur, “CFD analysis of artificially roughened solar air heater: a comparative study of C-Shape, reverse C-Shape, and reverse R-Shape roughness element,” *International Journal of Ambient Energy*, vol. 45, no. 1. Taylor and Francis Ltd., 2024. doi: 10.1080/01430750.2024.2331240.
[12] A. Agarwal, M. Ilunga, K. Tempa, and B. K. Humagai, “CFD Analysis of Solar Air Heater Using V-Shaped Artificial Roughness to Attain Heat Transfer Enhancement,” *International Journal of Energy Production and Management*, vol. 9, no. 3. International Information and Engineering Technology Association, pp. 171–180, 2024. doi: 10.18280/ijepm.090306.
[13] F. R. Menter, “Two-equation eddy-viscosity turbulence models for engineering applications,” *AIAA J.*, vol. 32, no. 8, pp. 1598–1605, Aug. 1994, doi: 10.2514/3.12149.
[14] M. Kaplan, “Augmented heat transfer in the solar air heater having hybrid roughness as continuous and discrete V ribs with dimples: a CFD analysis,” *Case Stud. Therm. Eng.*, vol. 77, p. 107548, Jan. 2026, doi: 10.1016/j.csite.2025.107548.
[15] V. S. Hans, R. P. Saini, and J. S. Saini, “Heat transfer and friction factor correlations for a solar air heater duct roughened artificially with multiple v-ribs,” *Sol. Energy*, vol. 84, no. 6, pp. 898–911, Jun. 2010, doi: 10.1016/j.solener.2010.02.004.
[16] S. Chaurasia, V. Goel, and A. Debbarma, “Impact of hybrid roughness geometry on heat transfer augmentation in solar air heater: A review,” *Solar Energy*, vol. 255. Elsevier Ltd, pp. 435–459, 2023. doi: 10.1016/j.solener.2023.02.052.
[17] A. Hassan, A. M. Nikbakht, S. Fawzia, P. Yarlagadda, and A. Karim, “A Comprehensive Review of the Thermohydraulic Improvement Potentials in Solar Air Heaters through an Energy and Exergy Analysis,” *Energies*, vol. 17, no. 7. Multidisciplinary Digital Publishing Institute (MDPI), 2024. doi: 10.3390/en17071526.
[18] A. Kocer, “Numerical investigation of heat transfer and thermo-hydraulic performance of solar air heater with different ribs and their machine learning-based prediction,” *Journal of the Brazilian Society of Mechanical Sciences and Engineering*, vol. 46, no. 2. Springer Science and Business Media Deutschland GmbH, 2024. doi: 10.1007/s40430-023-04663-3.
[19] U. F. Alqsair, “Numerical Simulation and Optimization of a Chevron-Type Corrugated Solar Air Heater,” *Energies*, vol. 18, no. 7. Multidisciplinary Digital Publishing Institute (MDPI), 2025. doi: 10.3390/en18071821.
[20] A. Kumar, R. P. Saini, and J. S. Saini, “A review of thermohydraulic performance of artificially roughened solar air heaters,” *Renewable and Sustainable Energy Reviews*, vol. 37. Elsevier Ltd, pp. 100–122, 2014. doi: 10.1016/j.rser.2014.04.063.
[21] A. Kumar, D. Kumar, and A. Layek, “Determination of Nusselt Number Over Artificially Roughened Solar Air Heater Using Numerical Approach,” *Lecture Notes in Mechanical Engineering*. Springer Science and Business Media Deutschland GmbH, pp. 483–492, 2021. doi: 10.1007/978-981-33-4165-4_45.
[22] A. S. Yadav and J. L. Bhagoria, “A numerical investigation of square sectioned transverse rib roughened solar air heater,” *International Journal of Thermal Sciences*, vol. 79. pp. 111–131, 2014. doi: 10.1016/j.ijthermalsci.2014.01.008.
[23] K. Kumar, D. R. Prajapati, and S. Samir, “Determination of effective efficiency of artificially roughened solar air heater duct using ribs,” *Distributed Generation and Alternative Energy Journal*, vol. 30, no. 2. Taylor and Francis Inc., pp. 57–77, 2015. doi: 10.1080/21563306.2015.11432421.

[24] J. L. Bhagoria, J. S. Saini, and S. C. Solanki, “Heat transfer coefficient and friction factor correlations for rectangular solar air heater duct having transverse wedge shaped rib roughness on the absorber plate,” *Renewable Energy*, vol. 25, no. 3. pp. 341–369, 2002. doi: 10.1016/S0960-1481(01)00057-X.
[25] N. Madhwesh, K. V. Karanth, and S. Kumar, “Heat transfer enhancement of a solar air heater using capsule-shaped turbulators: a numerical analysis,” *Scientific Reports*, vol. 15, no. 1. Nature Research, 2025. doi: 10.1038/s41598-025-99294-0.
[26] S. P. Shetty, N. Madhwesh, and K. Vasudeva Karanth, “Numerical analysis of a solar air heater with circular perforated absorber plate,” *Solar Energy*, vol. 215. Elsevier Ltd, pp. 416–433, 2021. doi: 10.1016/j.solener.2020.12.053.